Available online at www.sciencedirect.com
SCIENCE DIRECT®
Environmental Toxicology and Pharmacology 17 (2004) 129–141
ENVIRONMENTAL TOXICOLOGY AND PHARMACOLOGY ETAP
www.elsevier.com/locate/etap

Comparison of cytopathological changes induced by mercury chloride exposure in renal cell lines (VERO and BGM)

D. Romero [a], M. Gómez-Zapata [b], A. Luna [b], A.J. García-Fernández [a,*]

[a] *Department of Toxicology, School of Veterinary Medicine, University of Murcia, Espinardo Campus, E-30100 Murcia, Spain*
[b] *Department of Legal Medicine, School of Medicine, University of Murcia, Espinardo Campus, E-30100 Murcia, Spain*

Received 10 October 2003; accepted 31 March 2004

Abstract

The response to mercury chloride was assessed in two cell lines of renal origin, determining the range of toxic concentrations by Neutral Red assay after 24-h of exposure. Morphological changes in the Buffalo Green Monkey (BGM) and VERO cell lines after exposure to subcytotoxic doses (0.045 and 0.038 mM, respectively) equivalent to EC10 (effective concentrations 10%) of mercury chloride were evaluated at the structural and ultrastructural level by optic, transmission and scanning microscopy. Using transmission electron microscopy, the most notable findings in treated cells were the presence of intracytoplasmic inclusion bodies and apoptotic bodies. Scanning microscopy pointed to a cell with a disrupted perinuclear region and a decreased number of surface microvilli. Similar alterations in both in vivo and in vitro experiments have been described by other authors. We conclude that BGM and VERO renal cell lines can be considered as useful tools for toxicological studies involving mercury chloride.

Keywords: BGM and VERO cells line; Cytotoxicity; Mercury; Ultrastructural alterations; Microscopy

1. Introduction

Cell culture methods have been widely used in toxicological studies, primarily in basal cytotoxicity assays, the results of which can be used to design more specific studies. This development is due to new cell lines being introduced and for better characterisation of established cell lines (Zimmerhackl et al., 1998). Heavy metal toxicity, for example, has been assessed in vitro using renal, hepatic, nervous and other cell cultures, including tumour cells.

Mercury is present in the environment mainly as a result of human activity and is considered one of the most toxic of heavy metals. Most harmful are the organic mercury compounds; inorganic mercury, as in mercury chloride, is less toxic, but exerts specific renal toxicity. Its harmful effect on human and animal health has led to the development of many analytical and experimental procedures designed to determine the severity of such effects and its concentration in biological samples (Magos and Cernik, 1969; Farant et al., 1981; Shrivastava and Tandon, 1982; Bencko et al., 1986; Rodriguez Pereiro et al., 1998).

Structural and ultrastructural cell alterations induced by mercury exposure are among the most important aspects to have been studied. Several animal species, doses, techniques and exposure times have been used both in in vivo (Verity and Brown, 1970; Ganote et al., 1975; Ware et al., 1975; Hinglais et al., 1979; Andreev, 1991; Chavez et al., 1994; Lauwerys, 1994) and in vitro models (Bracken et al., 1984; Lachapelle et al., 1993; Chandler et al., 1994; Bucio et al., 1995; Wang and Pfeiffer, 2001). Lysosomes, mitochondria, membranes and the nucleus have been described as mercury accumulation zones (Norseth, 1968; Verity and Brown, 1970; Ware et al., 1975; Cherian and Nordberg, 1983; Zalups et al., 1993), while the labilization of membranes of intracellular organelles, such as lysosomes, peroxysomes and mitochondria (Lauwerys and Buchet, 1972; Roels et al., 1974) and DNA damage (Nakazawa et al., 1975; Kasschau and Meyn, 1981; Cantoni et al., col., 1984; Choi and Kim, 1984), represents the most frequently observed alteration induced by mercury.

* Corresponding author. Tel.: +34-968-367021; fax: +34-968-363417.
E-mail address: ajgf@um.es (A.J. García-Fernández).

1382-6689/$ – see front matter © 2004 Elsevier B.V. All rights reserved.
doi:10.1016/j.etap.2004.03.007

Several authors have suggested that metals such as mercury produce reactive oxygen species (ROS), which results in lipid peroxidation (Fukino et al., 1984). Moreover, mercury has been described as causing decreased levels of GSH in renal tubules with a concomitant decrease in SOD, Gpx and catalase activity, supporting the involvement of ROS in altering membrane integrity and as the mechanism that determines the nephrotoxic effects of mercury (Stohs and Bagchi, 1995). We have previously observed how the antioxidant mechanisms of CHO-K1 cells responded similarly to low doses (EC6.25) of cadmium and mercury and how the cytotoxicity parameters were also similar for both metals (García-Fernández et al., 2002).

BGM and VERO are two cell lines of renal origin, which have not been used very much in toxicological studies, especially for heavy metal assessment (Romero et al., 2003a,b). Both cell lines, however, have been used in influential microbiological studies (Yu et al., 2000; Drosten et al., 2003). As regards toxicological matter, the BGM cell line has only been mentioned in studies of dysentery caused by shellfish poisoning (DSP) (Croci et al., 1997). VERO has been used in studies of botulism (Haug et al., 2003) and Shiga's poisoning (Ishikawa et al., 2003). In previous studies in our laboratory (Romero et al., 2003a,b), both cell lines manifested a response to cadmium and/or lead similar to that of other cell lines of renal origin and were therefore be considered as alternative models for such toxicological studies.

In the present work, the morphological in vitro mercury-induced response to subcytotoxic doses of mercury chloride has been assessed to ascertain its suitability for future toxicological research. Two cell lines of renal origin (BGM and VERO) were used and the basal cytotoxicity was assessed using the Neutral Red assay (Borenfreund and Puerner, 1984) after 24 h of exposure to mercury chloride. A subcytotoxic dose equivalent to the EC10 was used for microscopic evaluation (0.045 and 0.038 mM for BGM and VERO, respectively).

2. Material and methods

2.1. Cell cultures

The BGM and VERO cell lines (from *Cercopitecus aethiops*) were obtained from the Cell Bank of the Tissue Culture Service of the University of Murcia. Both cell lines were cultured in Eagle's minimum essential medium (MEM, Sigma) supplemented with 10% (v/v) foetal calf serum (FCS), 100 IU penicillin/ml and 100 μg streptomicyn/ml. Cells were sown in 75-cm^2 bottles at a density of 1.5×10^4 cells/cm^2 and incubated at 37 °C in a CO_2 (5%) humidified incubator. The growth of both cell lines followed three well-defined growth phases: latent, exponential and stable, allowing us to identify the best moment for mercury chloride treatment (48 h after the beginning of subculture, just at the beginning of the exponential growth phase).

2.2. Test chemical

The mercury chloride was obtained from Sigma and a 5M stock solution was prepared in purified and sterilised water (Milli-Q). Solutions 10× for each concentration to be evaluated were daily prepared in MEM (Sigma) and refrigerated until use. These solutions were added to MEM to obtain the final concentrations. The MEM used in the control cultures was prepared in the same form but adding 10% purified water. Prior to carrying out the treatment, the osmolarity of these solutions (including the control) was measured so that any differences in cell viability after addition of the mercury chloride salt could be evaluated.

2.3. Neutral Red (NR) cytotoxicity assay

The cells were sown in 96-well microtitre plates, to which the mercury chloride was added 48 h later. The initial concentration range assayed was between 20 and 200 μM, while controls consisted of the medium with untreated cells and without cells. The cultures were tested using NR, which is selectively taken up by the lysosomes of living cells (Borenfreund and Puerner, 1984), thus pointing to the degree of viability. Twenty-four hours after the treatment, the medium containing mercury chloride was removed and NR solution was added to each well and incubated at 37 °C for 3 h. Cells were fixed with 0.5% (v/v) formaldehyde in 1% $CaCl_2$ solution and NR dye was eluted from the living cells using 100 μl acid alcohol (1% (v/v) acetic acid in 50% ethanol; Babich and Borenfreund, 1993). Absorbance was read on a Multiskan MCC/340P plate reader at 560 nm with a 690-nm reference filter. The mean absorbance for each concentration was expressed as a percentage of the value obtained for the blank wells and plotted against the mercury chloride concentration. The effective concentrations were determined from the dose–response curve by linear regression.

2.4. Optic microscopy

Cultures were evaluated every 24 h from the time of seeding until the end of each experiment, using a phase contrast inverter microscope Nikon Diaphot-TM.

2.5. Transmission electron microscopy (TEM)

The EC10 doses of mercury chloride (0.045 mM for BGM and 0.038 mM for VERO) were added 48 h after plating the cells were plated on 6-cm petri dishes at a density of 1.5×10^4 cells/cm^2. Three identical plates were prepared for each cell line. The cells were exposed to this toxic compound for 24 h at 37 °C. Control plates were prepared without mercury chloride. After exposure, the cells were trypsinised, collected and centrifuged (482 g, 10 min, +2 °C). The pellets were immediately fixed in 3% (v/v) glutaraldehyde, post-fixed in 1% (v/v) osmium tetroxide and stained with

4.8% uranyl acetate. After dehydration with a graded series of alcohol concentrations, the samples were rinsed in propylene oxide and impregnated with epoxy resins. The ultrathin sections (four for each plate) were contrasted with uranyl acetate and lead citrate for electron microscopy study. Electron micrographs were taken with a Zeiss EM 10C transmission electron microscope. The same process was carried out using non-treated VERO and BGM cell lines, preparing three plates for each cell line.

2.6. Scanning electron microscopy (SEM)

The cells were seeded in Leighton tubes and exposed to 0.045 and 0.038 mM of mercury chloride for BGM and VERO cell lines, respectively, for 24 h at 37 °C. They were then fixed in 3% (v/v) glutaraldehyde and post-fixed in 1% osmium tetroxide. Samples were dehydrated with a graded series of alcohol concentrations and 100% acetone. These were dried using an acetone–CO_2 bath in a $CPDO_2$ Balzers Union chamber. After sputtering with gold, images were taken with the Link-Isis program (Oxford Instruments, UK). Three Leighton tubes were seed for each cell line and for the treated and untreated cells.

2.7. Statistical analysis

Statistical analysis of the data were carried out using SPSS v10.0 statistical software (SPSS Inc., 1989–1999). Student's *t*-test was used to compare the cytotoxicity data between BGM and VERO cell lines. Dose–response curves were plotted using Sigma-Plot 8.0 software.

3. Results

3.1. Cytotoxicity assays

The mercury chloride concentration ranges, as measured by the NR assay, were 45–75 μM and 35–50 μM for BGM and VERO cell lines, respectively. The effective concentrations were obtained by linear regression from the corresponding dose–response curves (Fig. 1). The EC50 values obtained were 58 and 43 μM for BGM and VERO cell lines, respectively.

3.2. Morphological findings

3.2.1. Untreated cells

3.2.1.1. BGM cell line. Cells showed a typical epithelial morphology (Fig. 2a) with light and abundant cytoplasm occasionally containing small granules. The nucleus was circular and well-defined with 1–4 nucleoli. Giant multinucleated cells were occasionally seen. Transmission electron microscopy showed that the BGM cells were rounded, with a well-defined outline and a variable number of microvilli. Spherical or oval mitochondria with well-defined transversal cristae, abundant smooth endoplasmic reticulum, few phagolysosomes and clearly recognisable vacuoles were characteristic of this cell line. Abundant chromatin, scarce peripheral heterochromatin and one to four nucleoli were observed in the spherical or oval nuclei, which were situated in a central position in the cell (Fig. 2b). Scanning electron microscopy showed BGM cells to have

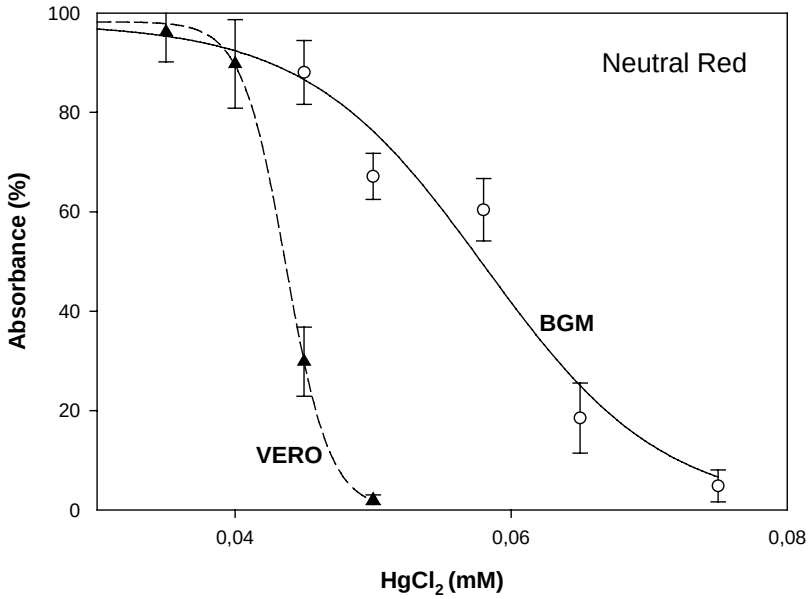

Fig. 1. Cytotoxicity curves of BGM and VERO cell lines exposed to $HgCl_2$. The cultures were tested using Neutral Red test 24-h after metal exposures (Babich and Borenfreund, 1993). Absorbance was read at 560 nm with a 690 reference filter (Bayoumi et al., 1999). The mean absorbance for each concentration was expressed as a percentage of the value obtained for the blank wells and plotted against the mercury chloride concentrations. Six observations were made for each concentration assayed.

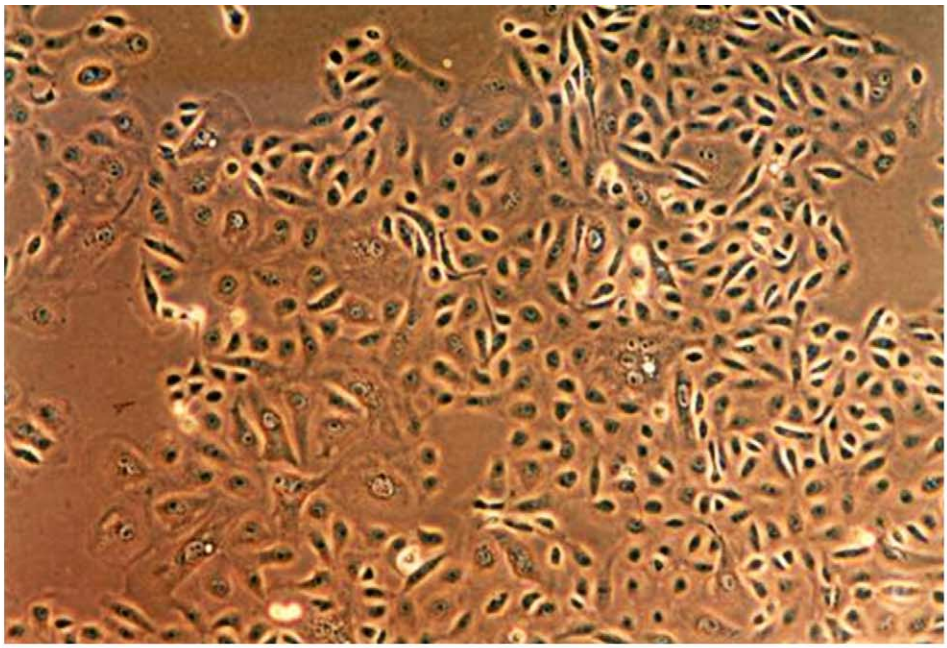

(a)

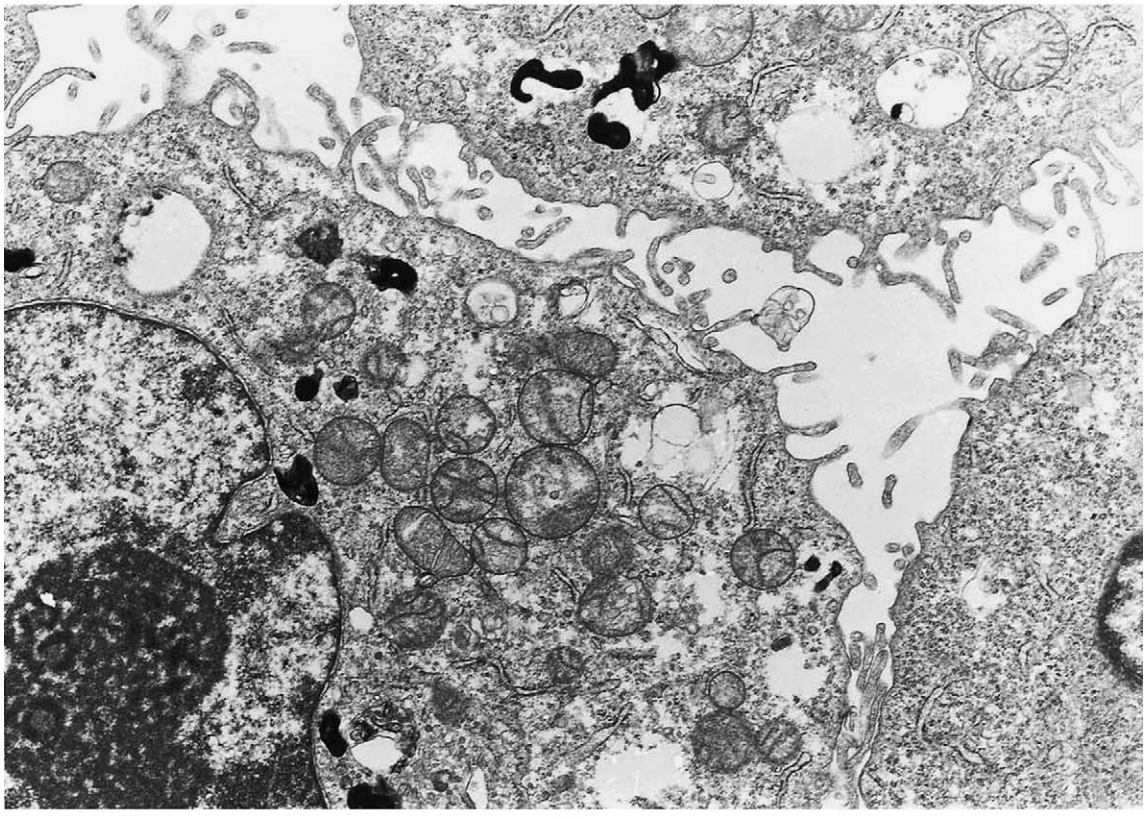

(b)

Fig. 2. Untreated BGM cells. (a) Cells with typical epithelial morphology, light and abundant cytoplasm, circular nucleus and well-defined nucleoli (MO, 100×). (b) Rounded cells, spherical and oval mitochondria, abundant smooth endoplasmic reticulum, few phagolysosomes, abundant chromatin and scarce heterochromatin (MET, 12,000×). (c) Abundant short microvilli over cell surface and perinuclear rupture (MEB, 2500×).

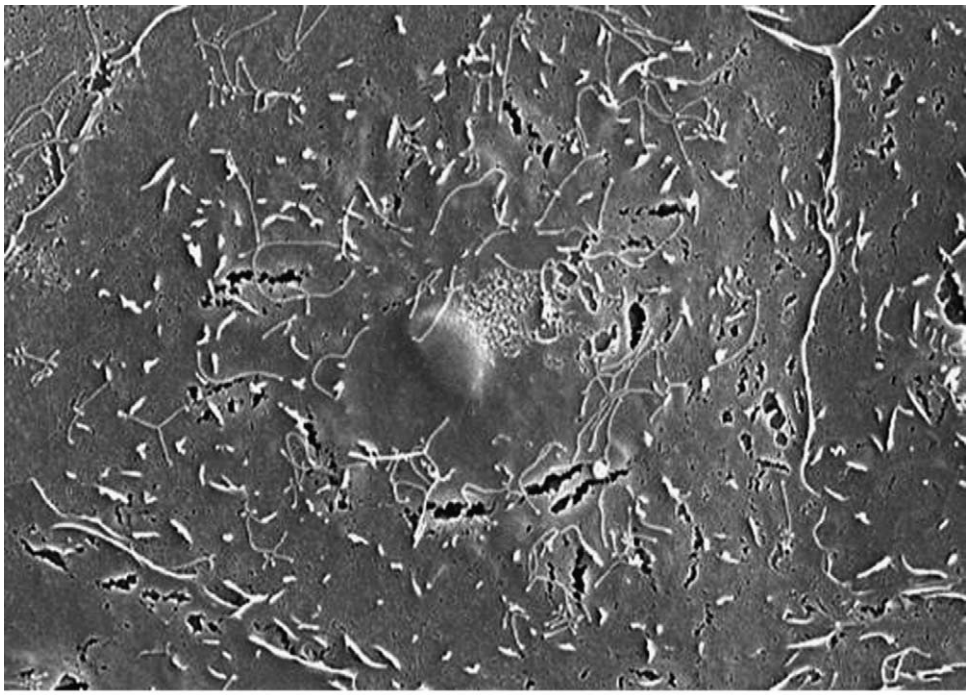

(c)

Fig. 2. (*Continued*).

an epithelial morphology with multiple nucleoli in a central nucleus. The nucleus/cytoplasm ratio was greatly in favour of the cytoplasm. Abundant short microvilli were evenly distributed over the cell surface, with the longest being observed around the nucleus. Perinuclear rupture was slight and probably resulted from to the method used (Fig. 2c).

3.2.1.2. VERO cell line. The VERO cells presented a variable morphology, fibroblastic and epithelial (Fig. 3a), with well-defined cell outlines and microvilli in variable but normally scarce quantities. The abundant cytoplasm volume showed well-recognisable organelles, but in smaller quantities than in the BGM cell line. Spherical or long mitochondria with transversal cristae were frequently situated near the nucleus. A nucleolus was observed in the irregular and elongated nucleus. Heterochromatin formed clumps and a large quantity of euchromatin could be seen. Free ribosomes were observed in the cytoplasm or associated to the endoplasmic reticulum. Autophagic inclusion bodies and vacuoles were also observed (Fig. 3b). Scanning electron microscopy showed BGM cells to have variable forms, although predominantly long with triangular forms also being common. The nucleus was oval with one or two nucleoli and surrounded by small, scarce ruptured cells. Surface microvilli varied in number, although in most cases they were few and sometimes absent. These microvilli were short, except those located near the nucleus (Fig. 3c).

3.2.2. Treated cells

3.2.2.1. BGM cell line. Optic microscopy (Fig. 4a) showed the cells to have cytoplasmic projections, intracytoplasmic vacuoles with different degrees of density and forming dark clumps near the apparently normal nucleus. Some cells were spherical with a lumpy nucleus and a scarce quantity of cytoplasm. Transmission electron microscopy (Fig. 4b) pointed to a high degree of cell tumefaction, although the cells maintained their original morphology with a circular or oval nucleus and a variable number of cytoplasmic projections unevenly distributed around the cells. An increased number of vacuoles, most of them large and occasionally with electrodense dots were observed. Autophagic inclusion bodies, myelin figures and concentric multilaminar phagolysosomes were commonly seen. Thin electrodense granules were evident in their interior. Condensed mitochondria ones and with internal dense granules others were frequently seen. Chromatin distribution was similar to that described in untreated cells. Scanning electron microscopy (Fig. 4c) pointed to smaller and fewer surface filaments than in untreated cells. In most of the treated cells cell rupture around the nucleus was a common alteration.

3.2.2.2. VERO cell line. Optic microscopy (Fig. 5a) showed cells with a morphology very similar to that of the control cells although some had an irregular outline and showed cytoplasmic projections and intense cytoplasmic vacuolisation. The nuclei ran from normal looking to

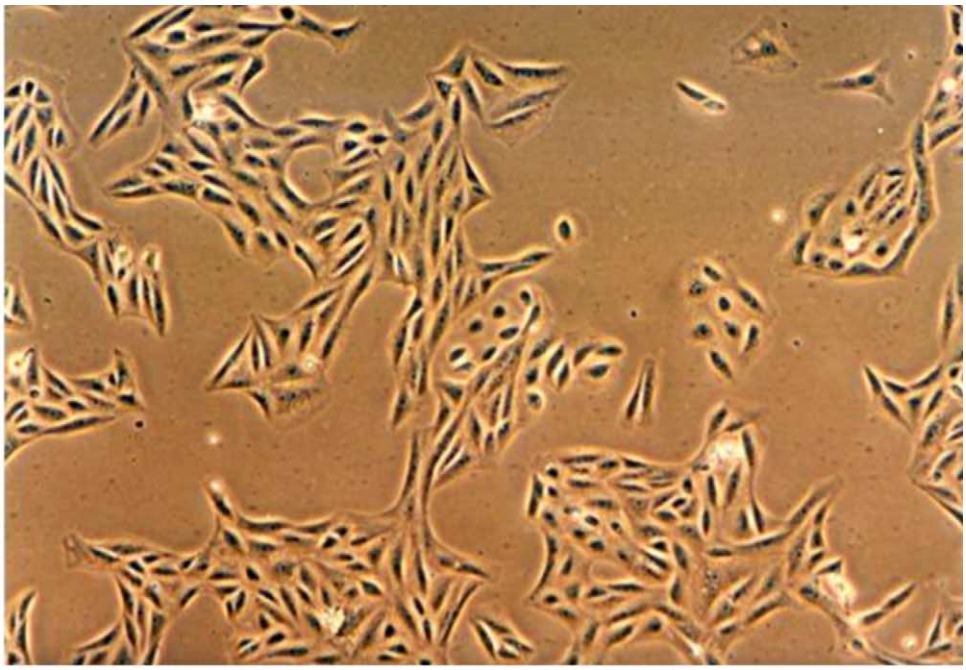

(a)

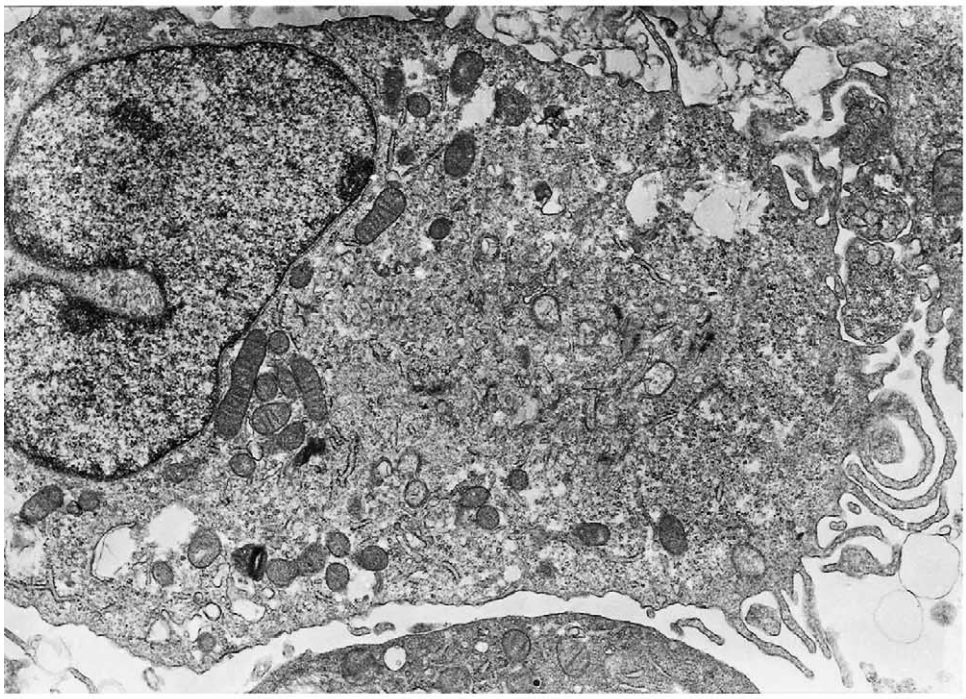

(b)

Fig. 3. Untreated VERO cells. (a) Fibroblastic and epithelial morphology and abundant cytoplasm volume (MO, 100×). (b) Spherical and long mitochondria near the nucleus, free ribosomes in the cytoplasm or associated to the endoplasmic reticulum and large quantity of euchromatin (MET, 11,000×). (c) Fibroblastic morphology and variable surface microvilli (MEB, 5900×).

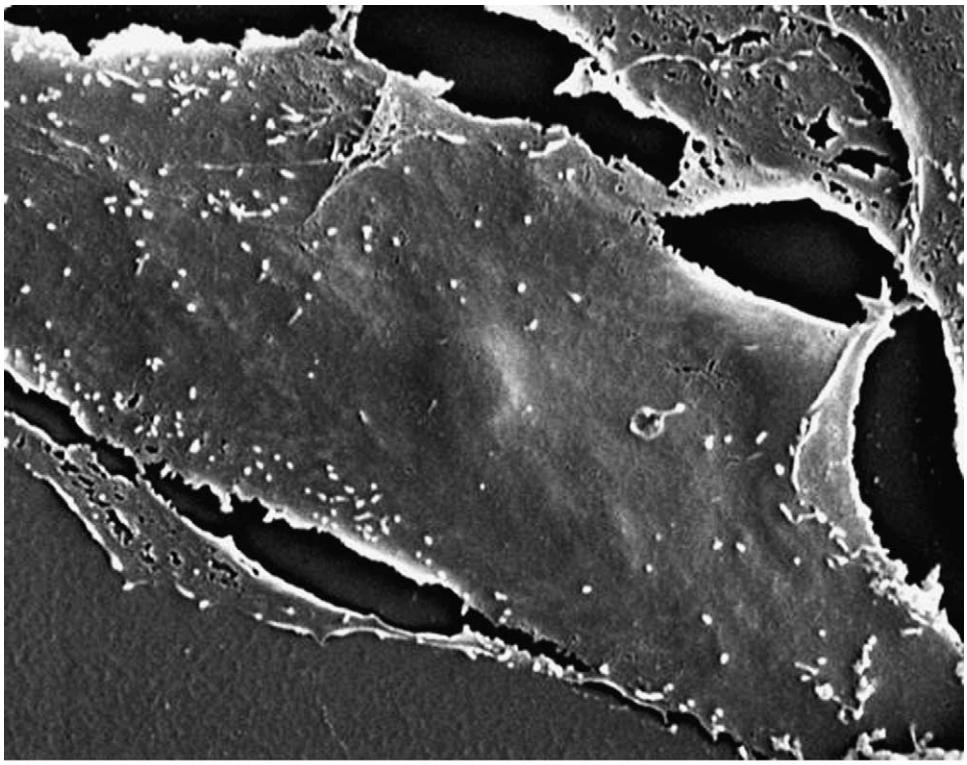

(c)

Fig. 3. (*Continued*).

diffuse. Some nucleoli were difficult to see. Some cells had a circular morphology with a refringent halo having lost their internal structure appearing as differently coloured stains. Transmission electron microscopy (Fig. 5b) showed tumefacted cells with necrosis being the prominent form of cell death. The cytoplasm appeared as a mottled, lumps diffuse mass distributed throughout the cytosol, with dense lysosomes and myelin figures, also in the mitochondria. The intranuclear euchromatin was dispersed and the heterochromatin formed peripheral clumps. The cytoplasmic processes were short and few in numbers. Scanning electron microscopy (Fig. 5c) showed cells with a very irregular outline containing a great quantity of lumps. The vacuoles were scarce in number and located around the internal side of the cytoplasmic membrane. A nucleus and nucleoli were evident. Small zones with ruptured membrane were observed and a characteristic feature was the low number of surface microvilli in the affected cells.

Table 1
Mercury chloride effective concentration 50% in several cell lines and primary cultures

Cells	EC50[a]	CA	ET	References
CHO[b] (hamster ovary)	3.3	NR	24	Bayoumi et al. (1998)
LLC-PK1[b] (*pig kidney*)	*9.4*	NR	*24*	Bohets et al. (1995)
WRL68[b] (human fetal liver)	9.6	BT	24	Bucio et al. (1995)
TG2[b] (rainbow trout gonad)	12	NR	24	Bayoumi et al. (1999)
BG/F[b] (fish epithelium)	16.5	NR	24	Babich et al. (1990)
BF2[b] (bluegill fry caudal trunk)	19	NR	24	Bayoumi et al. (1999)
HEP G2[b] (hepatome)	30.8	NR	24	Bohets et al. (1995)
I-407[b] (human intestinal epithelium)	32	NR	48	Keogh et al. (1994)
RPTC[c] (*rabbit kidney*)	*34.2*	*BT*	*24*	Aleo et al. (1992)
VERO[b] (*monkey kidney*)	*43*	*NR*	*24*	*This study*
SAOS[b] (osteoblastes)	48.2	NR	24	Bohets et al. (1995)
BGM[b] (*monkey kidney*)	*58*	*NR*	*24*	*This study*
MDCK[b] (*canine kidney*)	*83.6*	*NR*	*24*	Bohets et al. (1995)
HPTC[c] (*human kidney*)	*144*	*NR*	*24*	Bohets et al. (1995)

Renal cell lines are shown in italics.

[a] Effective concentration 50% of mercury chloride (μmol): T, cytotoxicity assay; ET, exposure time (h).

[b] Cell line.

[c] Primary culture: NR, Neutral Red; BT, Blue Tripan.

4. Discussion

Both cell lines presented a very similar response to mercuric chloride (Fig. 1). The fact that EC50 in both cell lines is midway between the values found for other cultures (Babich et al., 1990; Aleo et al., 1992; Bohets et al., 1995; Bucio et al., 1995; Bayoumi et al., 1999) underlines the usefulness of the cell lines for the proposed assays (Table 1).

The fact that apparently altered cells were observed in all the assays next to apparently normal cells and others that were dead confirms that the concentration chosen for the study was suitable for evaluating the critical point for cell survival. The frequency with which apparently altered cells could be seen varied with the cell line assayed, being more common in VERO. Since the technique used did not evaluate cell death but the percentage of viable cells, regardless of

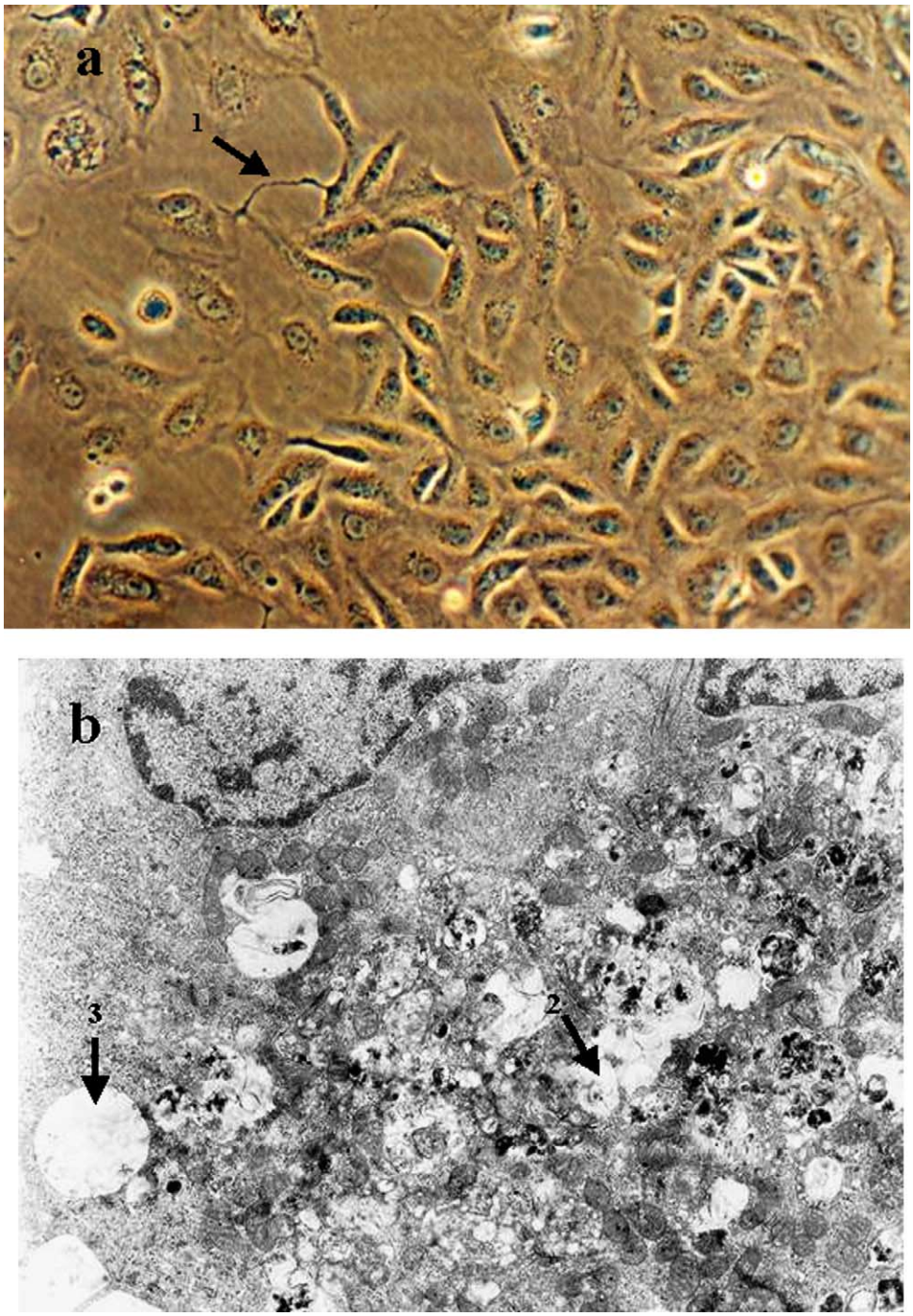

Fig. 4. Treated BGM cells. (a) Dendritic processes (arrow 1), intracytoplasmic vacuoles and forming dark clumps (MO, 100×). (b) Cellular tumefaction (arrow 2), variable number of cytoplasm projections and increased number of vacuoles (arrow 3) (MET, 11,000×). (c) Smaller and fewer surface filaments (arrow 4) and cell rupture around the nucleus (arrow 5) (MEB, 1900×).

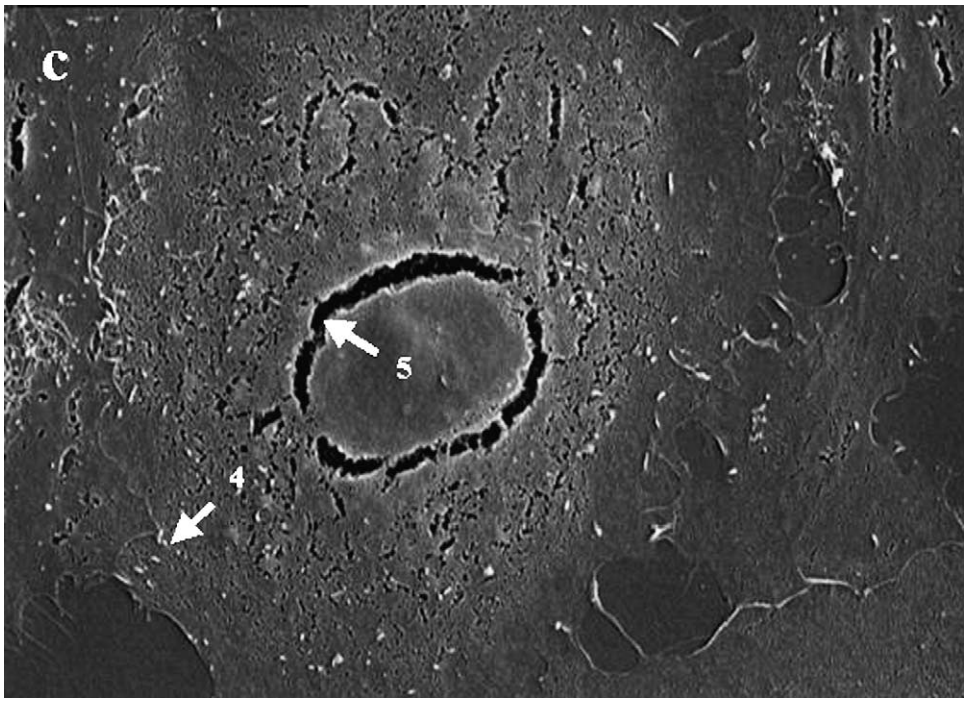

Fig. 4. (*Continued*).

the degree of alteration, we conclude that each cell line showed a different response to mercury chloride. The greater sensitivity of VERO was evident when EC10 ($T = 5.896$; $P < 0.001$) and EC50 ($T = 16.009$; $P < 0.001$) values were compared between both cell lines, and may explain this different way of manifesting the morphological effects. The vacuolisation of the cytoplasm was the morphological alteration that most closely reflected the results obtained by other authors (Ware et al., 1975; Bracken et al., 1984), which once again underlines the suitability of these cultures for visualising the effects of mercury at cell level.

Transmission electron microscopy showed that the alterations provoked by this metal leads to the death of some cells by necrosis, while there was no evidence of apoptosis phenomena. However, some cells in BGM showed a certain degree of cytoplasmic disorganisation and large vacuoles, although the nucleus could not be distinguished. Mercury is a metal capable of inducing apoptosis in cell cultures (Duncan-Achanzar et al., 1996; Shenker et al., 1997; Goering et al., 1999) and experimental animals (Nagashima et al., 1996). According to Duncan-Achanzar et al. (1996), the appearance of necrosis or apoptosis in renal cell cultures (LLC-PK1) depends on the concentration of the metal used. BGM was previously described as a cell line in which a cadmium-induced apoptotic phenomenon was evident (Romero et al., 2003a). It is possible that treated cells from the BGM line in our study are to be found in an unspecified state of apoptosis. Perhaps, for this process to develop a longer exposure time to the metal is necessary or, simply the process begins later. Further studies are required before it can be concluded that mercury chloride induces apoptosis in this cell line.

The alterations found at ultrastructural level were similar to those observed by other authors (Lachapelle et al., 1993; Bucio et al., 1995), although they showed what might be considered a later state of development. This could be explained by the fact that what the above authors considered "low doses" were well below what we considered to be low. For example, while Lachapelle et al. (1993) considered as a low doses a concentration of $HgCl_2$ equivalent to the concentration having no observable effect (NOEL), Bucio et al. (1995) considered as low a concentration almost twenty times more diluted than the EC50 and 6 times more diluted than that corresponding to NOEL, while considering as high doses a concentration 1.92 times more diluted than the EC50 and 1.7 times more concentrated than the NOEL. Other authors have considered as subcytotoxic a concentration of up to 850 times more dilute than the EC50 (Aleo et al., 1992). The effective concentration dose used by us (EC10) was between 1.1 and 2.7 times more dilute than the EC50 (depending on the cell line) and 1.1–2.1 times more concentrated than the NOEL. Our doses were nearer those that Bucio et al. (1995) considered high. This explains why our findings seem more pronounced than those of the above authors at low doses, although they do seem to follow the same pattern of toxicity, since the alterations were the same. Taken as a whole, the results lend weight to the assertions of some authors (Bracken et al., 1984; Bracken and Sharma, 1985), that mercury is a metal that progressively exhibits high levels of toxicity in renal cells during culture.

The presence of lysosomes with an electrodense content and vacuoles with a microgranular content, sometimes associated with myelin figures, suggests that the metal is initially encapsulated as part of cell defense mechanism. The presence of these microgranules throughout the cytoplasm suggests that membranous organelle activity is subsequently altered to a certain extent. This would agree with the data obtained by other authors, who cite mercury as a metal that is accumulated in lysosomes and capable of labilising the membranes of the cytoplasmic organelles, such as lysosomes, mitochondria and peroxisomes (Lauwerys and Buchet, 1972; Roels et al., 1974; Marigómez et al., 1996) and therefore, there is a the failure of the fagolysosome system forming part of the cell defense mechanism.

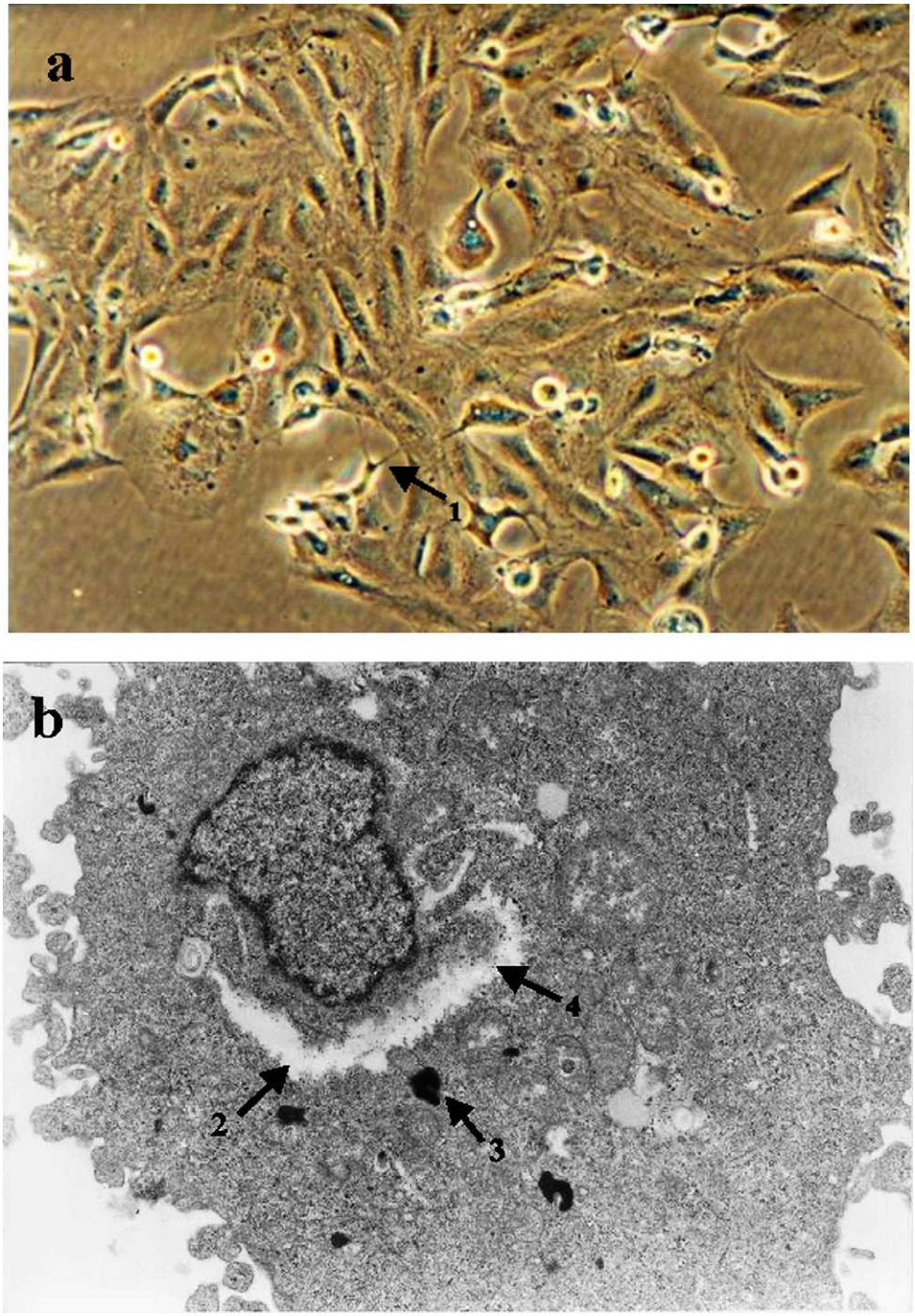

Fig. 5. Treated VERO cells. (a) Similar morphology to the control cells, processes cytoplasmic (arrow 1) and intense cytoplasmic vacuolisation (MO, 100×). (b) Tumefacted cells (arrow 2), dense lysosomes (arrow 3), diffuse lumps (arrow 4), myelin figures and heterochromatin with peripheral clumps (MET, 13,200×). (c) Irregular outline with great quantity of lumps (arrow 5) and small zones with ruptured membrane (arrow 6) (MEB, 1300×).

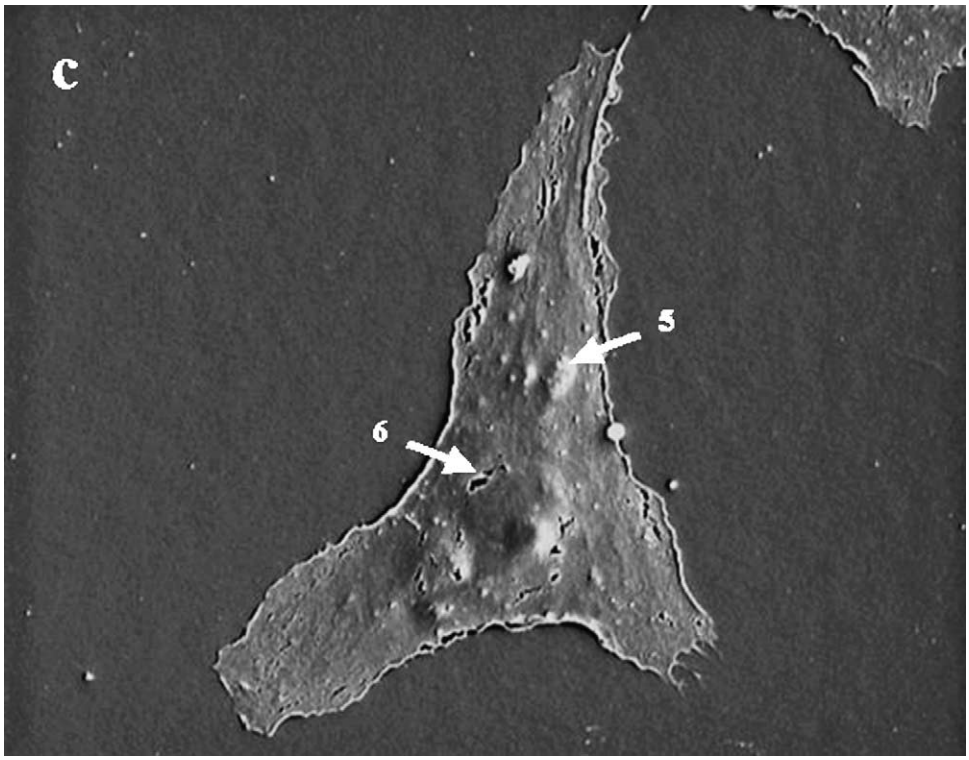

Fig. 5. (*Continued*).

A high degree of tumefaction was observed in both cell lines as a consequence of the hydric shock provoked by the mercury, and this may be the trigger of all the alterations observed at cell level. Indeed, some authors have pointed to this hydric shock as being responsible for the subsequent diminution in cell viability, rather than the direct interaction of mercury with cell components (Bracken et al., 1984; Bracken and Sharma, 1985; Miura and Imura, 1987). A time-dependent evaluation is necessary to corroborate this hypothesis.

Another organelle type to show alteration was the mitochondria, which occasionally showed condensation and poorly defined outlines. It is known that the inorganic form of this metal has an affinity for the mitochondria, which make them an important intracellular target (Zalups et al., 1993). Histochemical studies by electronic microscopy have demonstrated that mercury may be found inside the mitochondria (Ware et al., 1975). In our study, such a presence was evident in both cell lines. On the other hand, the point made by Ghadialy (1982) should be borne in mind, namely that the size and density of the dense osmophilic granules increases with the increased transport of water and electrolytes.

In some cells, certain irregular structures could be seen in the nucleus, perhaps corresponding to inclusion bodies. Some authors have described how mercury can be accumulated in the nucleus in the same way as lead, bismuth, copper and aluminium (Cherian and Nordberg, 1983). It has been demonstrated that mercury produces damage in DNA (Nakazawa et al., 1975; Kasschau and Meyn, 1981; Cantoni et al., 1984; Choi and Kim, 1984), which may explain how this damage, besides direct membrane labilisation, directs the alterations in the rest of the cell. Other authors, on the other hand, have observed very little mercury inside the nucleus (Ware et al., 1975). Again, new studies are necessary to ascertain any relation between these structures and mercury.

SEM showed no important changes except the loss of surface microvilli and the appearance of some granularity at cytoplasmic level. This may be regarded as the general alterations produced by any cytotoxic agent, although the clumps may have a direct relation with the internal alterations taking place. Whatever the case, these alterations in the microvilli reflect that described by several authors after exposure to high and low doses (NOEL and EC100, respectively) of mercury chloride in vitro (Chandler et al., 1994; Romero et al., 2000). These authors pointed to alterations in the membranes, consisting of holes, which may be related with the fenestrations observed in the surface of many cells in our study.

In conclusion, the cell lines BGM and VERO show a similar response to the action of mercuric chloride, which is, at the same time, similar to the response seen in other cell lines and in animals. This makes the two lines useful for studying cell alterations caused by the action of mercury. The possible alteration of cells in apoptosis in the BGM line should be confirmed before carrying out follow-up studies of this phenomenon in vitro.

Acknowledgements

This project was supported by CICYT, project BCM2000-0284.

References

Aleo, M., Taub, M.L., Kostyniak, P.J., 1992. Primary cultures of rabbit renal proximal tubule cells III. Comparative cytotoxicity of inorganic and organic mercury. Toxicol. Appl. Pharmacol. 112, 310–317.

Andreev, V.P., 1991. Changen in the nucleoli of ephitelial cells of the kidney tubules in mercuric chloride-induced experimental kidney tubular necrosis. Biull. Eksp. Biol. Med. 111, 66–69.

Babich, H., Goldstein, S.H., Borenfreund, E., 1990. In vitro cyto- and genotoxicity of organomercurials to cells in culture. Toxicol. Lett. 50, 143–149.

Babich, H., Borenfreund, E., 1993. Applications of the Neutral Red cytotoxicity assay to risk assessment of aquatic contaminants: an overview. Environ. Toxicol. Risk Assessment 1179, 215–229.

Bayoumi, A.E., García Fernández, A.J., Ordóñez, C., Balaña Fouce, R., Ordóñez, D., 1998. Evolución de la citotoxicidad in vitro de insecticidas organoclorados y metales en la línea CHO-K1 usando cuatro métodos alternativos. Rev. Toxicol. 15, 73–78.

Bayoumi, A.E., Pérez-Pertejo, Y., Ordoñez, C., García-Fernández, A.J., Reguea, R.M., Balaña-Fouce, R., Ordoñez, D., 1999. Evaluación de la citotoxicidad de metales in vitro en las líneas celulares de peces BF-2 y RTG-2 por dos métodos alternativos. Rev. Toxicol. 16, 17–21.

Bencko, V., Geist, T., Arbetova, D., Dharmadikari, D.M., Svandova, E., 1986. Biological monitoring of environmental pollution and human exposure to some trace elements. J. Hyg. Epidemiol. Microbiol. Immunol. 30, 1–10.

Bohets, H.H., Van-Thielen, M.N., Van-Der-Biest, I., Van-Landeghem, G.F., D'Haese, P.C., Nouwen, E.J., De-Broe, M.E., Dierickx, P.J., 1995. Cytotoxicity of mercury compounds in LLC-PK1, MDCK and human proximal tubular cells. Kidney Int. 47, 395–403.

Borenfreund, E., Puerner, J.A., 1984. A simple quantitative procedure using monolayer culture for cytotoxicity assays (HTD/NR-90). J. Tissue Cult. Methods 9, 7–9.

Bracken, W.M., Sharma, R.P., 1985. Biochemical responsiveness of a bovine kidney cell line to inorganic mercury. Arch. Environ. Contam. Toxicol. 14, 509–515.

Bracken, W.M., Sharma, R.P., Bourcier, D.R., 1984. Cellular distribution of inorganic mercury and its relation to cytotoxicity in bovine kidney cell cultures. J. Toxicol. Environ. Health 13, 865–877.

Bucio, L., Souza, V., Albores, A., Sierra, A., Chávez, E., Cárabez, A., Gutierrez-Ruiz, M.C., 1995. Cadmium and mercury toxicity in a human fetal hepatic cell line (WRL-68 cells). Toxicology 102, 285–299.

Cantoni, O., Christie, N.T., Swann, A., Drath, D.B., Costa, M., 1984. Mechanism of $HgCl_2$ cytotoxicity in cultured mammalian cells. Mol. Pharmacol. 26, 360–368.

Chandler, J.E., Messer, H.H., Ellender, G., 1994. Cytotoxicity of gallium and indium ions compared with mercuric ion. J. Dent. Res. 73, 1554–1559.

Chavez, E., Zazueta, C., Bravo, C., Reyes-Vivas, H., Pichardo, J., Chavez, R., 1994. Captopril protection from the nephrotoxic effects of mercury. Gac. Med. Mex. 130, 134–138.

Cherian, M.G., Nordberg, M., 1983. Cellular adaptation in metal toxicology and metallothionein. Toxicology 28, 1–15.

Choi, B.H., Kim, R.C., 1984. The comparative effects of methylmercuric chloride and mercuric chloride upon DNA synthesis in mouse fetal astrocytes in vitro. Exp. Mol. Pathol. 41, 371–376.

Croci, L., Cozzi, L., Stacchini, A., De Medici, D., Toti, L., 1997. A rapid tissue culture for detection of okadaic acid and related compounds in mussels. Toxicon 35, 223–230.

Drosten, C., Gunther, S., Preiser, W., van der Werf, S., Brodt, H.R., Becker, S., Rabenau, H., Panning, M., Kolesnikova, L., Fouchier, R.A., Berger, A., Burguiere, A.M., Cinatl, J., Eickmann, M., Escriou, N., Grywna, K., Kramme, S., Manuguerra, J.C., Muller, S., Rickerts, V., Sturmer, M., Vieth, S., Klenk, H.D., Osterhaus, A.D., Schmitz, H., Doerr, H.W., 2003. Identification of a novel coronavirus in patients with severe acute respiratory syndrome. N. Engl. J. Med. 348, 1967–1976.

Duncan-Achanzar, K.B., Jones, J.T., Burke, M.F., Carter, D.E., Laird, H.E., 1996. Inorganic mercury chloride-induced apoptosis in the cultured porcine renal cell line LLC-PK1. J. Pharmacol. Exp. Ther. 277, 1726–1732.

Farant, J.P., Brissette, D., Moncion, L., Bigras, L., Chartrand, A., 1981. Improved cold-vapor atomic absorption technique for the microdetermination of total and inorganic mercury in biological samples. J. Anal. Toxicol. 5, 47–51.

Fukino, H., Hirai, M., Hsueh, Y.M., Moriyasu, S., Yamani, Y., 1984. Effect of zinc pretreatment on mercuric chloride induced lipid peroxidation in the rat kidney. Toxicol. Appl. Pharmacol. 73, 395–401.

Ganote, C.E., Reimer, K.A., Jennings, R.B., 1975. Acute mercuric chloride nephrotoxicity. An electron microscopic and metabolic study. Lab. Invest. 31, 633–647.

García-Fernández, A.J., Bayoumi, A.E., Pérez-Pertejo, Y., Motas, M., Reguera, R.M., Ordóñez, C., Balaña-Fouce, R., Ordóñez, D., 2002. Alterations of the glutathione-redox balance induced by metals in CHO-K1 cells. Comp. Biochem. Physiol. C 132, 365–373.

Ghadialy, F.N., 1982. Ultrastructural Pathology of the Cell and Matrix, second ed. Butterworths, London.

Goering, P.L., Thomas, D., Rojko, J.L., Lucas, A.D., 1999. Mercuric chloride-induced apoptosis is dependent on protein synthesis. Toxicol. Lett. 105, 183–195.

Haug, G., Leemhuis, J., Tiemann, D., Meyer, D.K., Aktories, K., Barth, H., 2003. The host cell chaperone Hsp90 is essential for translocation of the binary *Clostridium botulinum* C2 toxin into the cytosol. J. Biol. Chem., in press.

Hinglais, N., Druet, P., Grossetete, J., Sapin, C., Bariety, J., 1979. Ultrastructural study of nephritis induced in Brow Norway rats by mercury chloride. Lab. Invest. 41, 150–159.

Ishikawa, S., Kawahara, K., Kagami, Y., Isshiki, Y., Kaneko, A., Matsui, H., Okada, N., Danbara, H., 2003. Protection against Shiga toxin 1 challenge by immunization of mice with purified mutant Shiga toxin 1. Infect. Immun. 71, 3235–3239.

Kasschau, M.R., Meyn, R.E., 1981. Recovery of Chinese hamster cells from mercuric chloride exposure. J. Toxicol. Environ. Health 7, 9–18.

Keogh, J.P., Steffen, B., Siegers, C.P., 1994. Cytotoxicity of heavy metals in the human small intestinal epithelial cell line I-407: the role of glutation. J. Toxicol. Environ. Health 43, 351–359.

Lachapelle, M., Guertin, F., Marion, M., Fournier, M., Denizeau, F., 1993. Mercuric chloride affects protein secretion in rat primary hepatocytes cultures: a biochemical ultrastructural, and gold immunocytochemical study. J. Toxicol. Environ. Health 38, 343–354.

Lauwerys, R., 1994. In: Masson, S.A (Ed.), Toxicología Industrial e Intoxicaciones Profesionales. Barcelona.

Lauwerys, R., Buchet, J.P., 1972. Study on the mechanism of lysosome labilization by inorganic mercury in vitro. Eur. J. Biochem. 26, 535–542.

Magos, L., Cernik, A.A., 1969. A rapid method for estimating mercury in undigested biological samples. Br. J. Ind. Med. 26, 144–149.

Marigómez, I., Soto, M., Kortabitarte, M., 1996. Tissue-level biomarkers and biological effect of mercury on sentinel slugs, *Arion ater*. Arch. Environ. Contam. Toxicol. 31, 54–62.

Miura, K., Imura, N., 1987. Mechanism of methylmercury cytotoxicity. Crit. Rev. Toxicol. 18, 161–189.

Nagashima, K., Fujii, Y., Tsukamoto, T., Nukuzuma, S., Satoh, M., Fujita, M., Fujioka, Y., Akagi, H., 1996. Apoptotic process of cerebellar degeneration in experimental methylmercury intoxication of rats. Acta Neuropathol. 91, 72–77.

Nakazawa, N., Makino, F., Okada, S., 1975. Acute effects of mercuric compounds on cultured mammalian cells. Biochem. Pharmacol. 24, 489–493.

Norseth, T., 1968. The intracellular distribution of mercury in rat liver after a single injection of mercuric chloride. Biochem. Pharmacol. 17, 581–593.

Rodriguez Pereiro, I., Wasik, A., Lobinski, R., 1998. Purge-and-trap isothermal multicapillary gas chromatographic sample introduction accessory for speciation of mercury by microwave-induced plasma atomic emission spectrometry. Anal. Chem. 70, 4063–4069.

Roels, H., Buchet, J.P., Lauwerys, R., 1974. Comparative study of the labilization of lysosomes, peroxysomes and mitochondria by inorganic mercury in vitro. In: Reid, E. (Ed.), Methodological Developments in Biochemistry, Subcellular Studies, vol. 4. Longman, London.

Romero, D., Gómez-Zapata, M., Luna, A., García-Fernández, A.J., 2000. Utilidad de la línea celular de origen tumoral A-Mel-3 en la evaluación de la citotoxicidad por metales pesados. Rev. Toxicol. 17, 133–139.

Romero, D., Gómez-Zapata, M., Luna, A., García-Fernández, A.J., 2003a. Morphological characterisation of BGM (Buffalo Green Monkey) cell line exposed to low doses of cadmium chloride. Toxicol. In Vitro 17, 293–299.

Romero, D., Gómez-Zapata, M., Luna, A., García-Fernández, A.J., 2003b. Morphological characterization of renal cell lines (BGM and VERO) exposed to low doses of lead nitrate. Histol. Hitopathol. 19, 69–73.

Shenker, B.J., Datar, S., Mansfield, K., Shapiro, I.M., 1997. Induction of apoptosis in human T-cells by organomercuric compounds: a flow cytometric analysis. Toxicol. Appl. Pharmacol. 143, 397–406.

Shrivastava, A.K., Tandon, S.G., 1982. Studies on mercury pollution: microdetermination of mercury in biological materials by cold vapour atomic absorption spectrometry. Int. J. Environ. Anal. Chem. 11, 221–226.

Stohs, S.J., Bagchi, D., 1995. Oxidative mechanisms in the toxicity of metal ions. Free Radic. Biol. Med. 18, 321–336.

Verity, M.A., Brown, W.J., 1970. Hg^{2+} induced kidney necrosis. Subcellular localisation and structure-linked lysosomal enzyme changes. Am. J. Pathol. 61, 57.

Wang, A., Pfeiffer, C.J., 2001. Cytophatology induced by mercuric chloride and methylmercury in cultured renal cells of the Atlantic spotted dolphin (*Stenella plagiodon*). J. Submicrosc. Cytol. Pathol. 33, 7–16.

Ware, R.A., Burkholder, P.H., Chang, L.W., 1975. Ultrastructural changes in renal proximal tubules after chronic organic and inorganic mercury intoxication. Environ. Res. 10, 121–140.

Yu, M., Tang, Y., Guo, M., Zhang, Q., Saif, Y.M., 2000. Characterization of a small round virus associated with the poult enteritis and mortality syndrome. Avian Dis. 44, 600–610.

Zalups, R.K., Knutson, K.L., Schnellmann, R.G., 1993. In vitro analysis of the accumulation and toxicity of inorganic mercury in segments of the proximal tubule isolated from the rabbit kidney. Toxicol. App. Pharmacol. 119, 221–227.

Zimmerhackl, L.B., Momm, F., Wiegele, G., Brandis, M., 1998. Cadmium is more toxic to LLC-PK_1 cells than to MDCK cells acting on the cadherin–catenin complex. Am. J. Physiol. 275, 143–153.